Fitting Neurological Protein Aggregation Kinetic Data via a 2-Step, Minimal/"Ockham's Razor" Model: The Finke−Watzky Mechanism of Nucleation Followed by Autocatalytic Surface Growth†

Aimee M. Morris,‡ Murielle A. Watzky,‡ Jeffrey N. Agar,§ and Richard G. Finke*,‡

Department of Chemistry, Colorado State University, Fort Collins, Colorado 80523, and Department of Chemistry and Volen Center, Brandeis University, 415 South Street, Waltham, Massachusetts 02454

Received September 18, 2007; Revised Manuscript Received November 19, 2007

ABSTRACT: The aggregation of proteins has been hypothesized to be an underlying cause of many neurological disorders including Alzheimer's, Parkinson's, and Huntington's diseases; protein aggregation is also important to normal life function in cases such as G to F-actin, glutamate dehydrogenase, and tubulin and flagella formation. For this reason, the underlying mechanism of protein aggregation, and accompanying kinetic models for protein nucleation and growth (growth also being called elongation, polymerization, or fibrillation in the literature), have been investigated for more than 50 years. As a way to concisely present the key prior literature in the protein aggregation area, Table 1 in the main text summarizes 23 papers by 10 groups of authors that provide 5 basic classes of mechanisms for protein aggregation over the period from 1959 to 2007. However, and despite this major prior effort, still lacking are both (i) anything approaching a consensus mechanism (or mechanisms), and (ii) a generally useful, and thus widely used, simplest/"Ockham's razor" kinetic model and associated equations that can be routinely employed to analyze a broader range of protein aggregation kinetic data. Herein we demonstrate that the 1997 Finke−Watzky (F−W) 2-step mechanism of slow continuous nucleation, A → B (rate constant k_1), followed by typically fast, autocatalytic surface growth, A + B → 2B (rate constant k_2), is able to quantitatively account for the kinetic curves from all 14 representative data sets of neurological protein aggregation found by a literature search (the prion literature was largely excluded for the purposes of this study in order provide some limit to the resultant literature that was covered). The F−W model is able to deconvolute the desired nucleation, k_1, and growth, k_2, rate constants from those 14 data sets obtained by four different physical methods, for three different proteins, and in nine different labs. The fits are generally good, and in many cases excellent, with R^2 values ≥0.98 in all cases. As such, this contribution is the current record of the widest set of protein aggregation data best fit by what is also the simplest model offered to date. Also provided is the mathematical connection between the 1997 F−W 2-step mechanism and the 2000 3-step mechanism proposed by Saitô and co-workers. In particular, the kinetic equation for Saitô's 3-step mechanism is shown to be mathematically identical to the earlier, 1997 2-step F−W mechanism under the 3 simplifying assumptions Saitô and co-workers used to derive their kinetic equation. A list of the 3 main caveats/limitations of the F−W kinetic model is provided, followed by the main conclusions from this study as well as some needed future experiments.

Protein aggregation is known to be intimately associated with many different types of neurological disorders, including Alzheimer's, Parkinson's and Huntington's diseases (*1*−*3*). Understanding the underlying mechanism(s) of protein aggregation is, therefore, central to controlling and otherwise rationally dealing with this important aspect of the etiology of these neurological disorders. Indeed, protein aggregation has been postulated to be the underlying cause of such diseases (*4*−*14*), although cause and effect are still not unequivocally demonstrated and, therefore, remain controversial. Naturally occurring, non-disease state protein aggregation is also a part of normal life function in cases such as G to F-actin conversion (*15*−*18*), glutamate dehydrogenase (*19*−*22*), and tubulin (*16*, *18*) and flagella (*18*) formation. Hence, understanding especially the simplest description of the mechanism(s) of protein aggregation is critically important for both the aforementioned disease as well as non-disease states. For the above reasons, the basic mechanism(s) of protein aggregation has been the focus of considerable prior effort in at least 30 laboratories over a period of approximately 50 years (*23*).

† The F−W mechanism grew out of long-term support by DOE Grant SE-FG02-03ER15453; without that long-term support its discovery would not have been possible. Partial support by NSF Grant 0611588 is also gratefully acknowledged as is Grant ALSA 1392 to J.N.A.'s laboratories.

* Corresponding author. E-mail: rfinke@lamar.colostate.edu. Tel: (970) 491-2541. Fax: (970) 491-1801.

‡ Colorado State University.

§ Brandeis University.

10.1021/bi701899y CCC: $40.75
Published on Web 02/05/2008

Protein aggregation studies are generally acknowledged (*16*, *18*, *24*−*27*) to have begun in earnest with Oosawa's 1959 and 1962 studies of the G-actin to F-actin polymerization where G stands for the globular and F the fibril form of actin (*15*, *16*). In order to proceed rationally and in as best informed a mode as possible, we have recently constructed a critical review of the prior protein aggregation literature (*23*). We find that there are 5 basic classes of mechanisms for protein aggregation over the period from 1959 to 2007 (*23*). Those studies are listed in Table 1, Table 1 being the first of two key tables of prior work that is discussed in our forthcoming critical review (*23*). The essence of Table 1 directly relevant to the present contribution is as follows: (i) the most cited, "complete" mechanism is the subsequent monomer addition mechanism, Scheme 1 (*16*, *17*, *28*, *29*); and (ii) the resulting mathematics and kinetic equations corresponding to the complete mechanism are, however, not routinely used to fit experimental data (*25*, *26*, *28*, *29*). Alternatively, when fits are possible (following numerous assumptions and approximations (*16*, *18*, *27*)), the resultant equation obfuscates verification (or refutation) of whether nucleation and then growth are present and deconvolutable (growth also being called polymerization, elongation, or "heterogeneous nucleation" in some treatments[1]). The deconvolution of nucleation from growth is key since these are central concepts in the broader literature of aggregation phenomenon in Nature (*23*, *30*−*33*). In addition our review of the literature (*23*) reveals that (iii) nothing approaching a consensus mechanism—or even an accepted primary model for fitting data—has emerged; and especially important for the present work (iv) a simplest possible, "Ockham's razor" model (*34*) that can be used to fit experimental data has not appeared, even though mechanistic scientists know that an Ockham's razor approach to mechanism is an essential part of rigorous mechanistic science. Finally, also sorely lacking is (v) a minimal model that can routinely and successfully be used for the badly needed deconvolution of nucleation from growth[1] for a broad range of kinetic data, even if that minimal model is, by necessity, phenomenological and unsophisticated relative to a more "complete" mechanism.

Herein we report the following results and insights: (i) that the 1997 Finke−Watzky (hereafter F−W)[2] 2-step mechanism (*31*) of slow, continuous nucleation followed by typically fast autocatalytic surface growth,[3] Scheme 2 and Figure 1 with its associated rate law, eq 1, and analytic equation, eq 2, is able to fit all of the 14 representative protein aggregation data sets we have been able to mine out of the (non-prion) neurological protein aggregation and related literature; (ii) that those in general excellent, often seemingly best-to-date fits demonstrate the broad applicability of the F−W mechanism to amyloid, α-synuclein, and polyglutamine disease proteins; and (iii) that the F−W mechanism is both the simplest ("Ockham's razor" (*34*)) model yet reported and perhaps the simplest conceivable model (see Scheme 2), for protein aggregation that is also able to fit a wide body of protein aggregation data. In addition, we report (iv) that the F−W mechanism achieves the key result of deconvoluting the crucial nucleation step from the growth step,[1] and we also show herein (v) that the 3-step mechanism proposed in 2000 by Saitô and co-workers (*35*) (entry 10 of Table 1) yields, after the necessary simplification and assumptions those authors made to make the mathematics manageable, a kinetic equation that we demonstrate herein is mathematically identical to the simpler, 2-step F−W mechanism published 3 years earlier (*31*).

Scheme 1: The Subsequent Monomer Addition Mechanism for the Aggregation of Proteins

$$P_1 + P_1 \underset{k_{-1}}{\overset{k_1}{\rightleftharpoons}} P_2$$
$$P_1 + P_2 \underset{k_{-2}}{\overset{k_2}{\rightleftharpoons}} P_3$$
$$P_1 + P_i \underset{k_{-i}}{\overset{k_i}{\rightleftharpoons}} P_{i+1}$$

Scheme 2: The F−W Mechanism (*31*) for Nucleation and Growth Phenomenon[a]

$$A \xrightarrow{k_1} B$$
$$A + B \xrightarrow{k_2} 2B$$

[a] This mechanism was first worked out for transition-metal nanocluster nucleation and growth (*31*, *32*) (for a more expanded list of references on nanoclusters, please refer to the Supporting Information), but this work as well as another in progress (33) shows that it also applies to other larger particle and aggregate formation phenomenon in Nature. Note that (i) the resultant kinetic curves are generally sigmoidal (see Figure 1); (ii) the A → B and A + B → 2B steps are typically composites of what may be hundreds to even thousands of actual elementary steps (*31*, *32*) (e.g., those back in Scheme 1). Hence, the resultant rate constants, k_1 and k_2, are necessarily average values of all the underlying steps.

$$\frac{-\mathrm{d[A]}}{\mathrm{d}t} = k_1[\mathrm{A}] + k_2[\mathrm{A}][\mathrm{B}] \quad (1)$$

$$[\mathrm{A}]_t = \frac{\dfrac{k_1}{k_2} + [\mathrm{A}]_0}{1 + \dfrac{k_1}{k_2[\mathrm{A}]_0}\exp(k_1 + k_2[\mathrm{A}]_0)t} \quad (2)$$

Finally, eq 3 will prove to be the most convenient form for analyzing all but one of the literature data sets reexamined

[1] The nomenclature in the protein aggregation literature is varied and can be confusing, with multiple terms being used for (we infer) more or less the same intended meaning. Specifically, for growth or agglomeration one also sees the terms "elongation", "aggregation", "fibrillation", and "polymerization". For the nucleation period one sees the phenomenological terms of "induction period" or "lag phase". Adding considerable confusion is the term "heterogeneous nucleation" used, we surmise, in the dictionary definition/meaning of heterogeneous as nucleation of "different" species, for example, new protein polymers on the surface of existing polymers. We would simply call this seeded autocatalytic growth. The confusion here arises since, traditionally *in the nucleation literature*, "heterogeneous nucleation" means nucleation occurring within a different phase (such as nucleation on a solid surface despite the reactants being soluble in solution). Herein we will use the terms (homogeneous) nucleation and (autocatalytic surface) growth as defined rigorously before and also herein by the kinetic equations and respective k_1 and k_2 rate constants in Scheme 2. One exception is in Table 1 where we retain the terms used by the original authors so as to properly represent and reproduce that literature.

[2] Abbreviations: CD, circular dichroism; DLS, dynamic light scattering; "*f*"= fraction of reaction completed; F−W = Finke−Watzky; ThT = TfT = Thioflavin T.

[3] Noteworthy is that the A + B → 2B step is the kinetic definition of autocatalysis, that is, a reaction in which a product (B) is also a reactant; this is why the curves "turn on" with almost step-function-like appearance in some cases with the middle part of the reaction going faster and faster (i.e., and until the reaction runs out of A, after which the reaction then slows down).

Table 1: Key Lead References from the Prior (Primarily Non-Prion) Literature of Protein Aggregation Mechanisms

Entry	Reference	Year	Title	Key Selected Contents
1	(15)	1959	G-F Transformation of Actin as a Fibrous Condensation	Oosawa and coworkers are pioneers in the field of protein polymerization with the recognition of actin polymerization of the general mechanism $n(\text{G-actin}) \overset{x\ Mg^{2+}}{\rightleftharpoons} (\text{F-actin})_n$, where G-actin is the globular and F-actin is the fibrous forms of actin. In 1959 they used the techniques of flow birefringence, light scattering, viscosity, and ultra-centrifugation as evidence for the fibrous condensation. In 1962, the aggregation of macromolecules with a focus on actin was proposed to aggregate by a helical rather than linear aggregation mechanism above a critical concentration of macromolecules. It was further proposed that F-actin is the helical aggregate of G-actin. The expression $\frac{dn_h}{dt} = [k_+\lambda(t) - k_-]\int [k_+'\lambda_3(t) - k_-'\lambda_{3h}(t)]dt + 3[k_+'\lambda_3(t) - k_-'\lambda_{3h}(t)] + k_-\lambda_{3h}(t)$, is given for the rate of total monomers participating in helical polymers, where n_h is the total number concentration of monomers participating in helical polymers, k_+ and k_- are the forward and reverse rate constants for attachment and detachment of monomers, $\lambda(t)$ is the number concentration of monomers, $k_+'\lambda_3(t)$ and $k_-'\lambda_{3h}(t)$ are the forward and reverse transformation rates of ordinary trimers to nuclei of helical polymers. This expression can only be approximately solved with a number of assumptions, but is an early and important contribution to the mechanisms of protein aggregation.
	(16)	1962	A Theory of Linear and Helical Aggregations of Macromolecules	
2	(19)	1971	Glutamate Dehydrogenase: Anatomy of a Regulatory Enzyme	Eisenberg was, to the best of our knowledge, the first to propose subsequent monomer addition as the (complete) mechanism for a protein aggregation system. In this case he examined the polymerization of glutamate dehydrogenase of the basic reaction, $n(\text{glutamate dehydrogenase}) \rightleftharpoons (\text{glutamate dehydrogenase})_n$. Of note is his recognition of similarities between protein aggregation phenomena and early polymerization literature. It was this recognition that allowed Eisenberg to propose in 1971 the mechanism shown to the left for the polymerization of glutamate dehydrogenase, where P_i is the polymerized species of weight M_i, and K_i is the equilibrium constant for the reaction, K_i being assumed to be the same for each monomer-addition step. $P_i + P_1 \overset{K_i}{\rightleftharpoons} P_{i+1}$
3			Mechanism of Bovine Liver Glutamate Dehydrogenase Self-Association	In 1975 and 1976, Eisenberg's subsequent monomer addition mechanism for glutamate dehydrogenase (entry 2) was questioned in a series of three papers. The basic driving force behind this series of papers is that the subsequent monomer addition mechanism cannot account for all of the experimental data in varying concentration ranges. Due to this fact, the authors propose a new mechanism for the polymerization of glutamate dehydrogenase termed the "random association" mechanism shown to the right. The "random association" mechanism means that two polymers of any size can come together and that the rate constants for this process are the same regardless of the size of P_i and P_j. This random aggregation mechanism was tested using previous aggregation data and also using quasi-elastic light scattering to measure to probe the kinetics of bovine liver glutamate dehydrogenase although, no aggregation kinetics along with a fit to the proposed mechanism are given. $P_i + P_j \rightleftharpoons P_{i+j}$ $i, j = 1, 2,...\infty$
	(20)	1975	I. Kinetic Evidence for a Random Association Mechanism	
	(21)	1975	II. Simulation of Relaxation Spectra for an Open Linear Polymerization Proceeding via a Sequential Addition of Monomer Units	
	(22)	1976	III. Characterization of the Association-Dissociation Stoichiometry with Quasi-elastic Light Scattering	

Table 1 (Continued)

Entry	Reference	Year	Title	Key Selected Contents
4	(17)	1975	Kinetics of the Cooperative Association of Actin to Actin Filaments	In 1975, Wegner and Engel proposed the subsequent monomer addition mechanism for actin fibril formation with the assumption that the rate constant for dimer formation would be different, but all subsequent rate constants would be equivalent. This proposed mechanism is shown on the left where A is an actin molecule, k_N and k_N' are the rate constants for the formation and destruction of the dimer, and k and k′ are the rate constants for the binding and dissociation of protomers in the so-called elongation steps. The associated differential equations are shown on the right where c_i represents the concentration of the i-mer with $\infty > i > 3$. Also determined in this 1975 work is a critical nucleus size of three or four. Their proposed mechanism was tested with experimental data, for the actin to actin filaments aggregation reaction, to demonstrate the mechanism's ability to account for the experimental data, and visually poor to fair fits were observed. 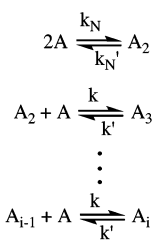 $\frac{dc_2}{dt} = k_N c_1^2 - k_N' c_2 - k c_1 c_2 + k' c_3$ $\frac{dc_i}{dt} = k c_1 c_{i-1} - k' c_i - k c_1 c_i + k' c_{i+1}$
5	(28)	1980	Kinetic Studies on Photolysis-Induced Gelation of Sickle Cell Hemoglobin Suggests New Mechanism	These authors propose an early word mechanism in 1980, and then a pictorial mechanism in 1985, for the polymerization of sickle hemoglobin, the basic stoichiometry of which is $n(hemoglobin - S) \rightarrow (hemoglobin - S)_n$. In 1980 the general mechanism for the polymerization process was given as shown on the left, essentially Eisenberg's monomer addition mechanism. This mechanism was examined in the classic and well studied sickle hemoglobin system; the proposed rate equations consist of double, so-called homogeneous and "heterogeneous," nucleation for the net polymerization process: $\frac{dc_P}{dt} = K_N k_+ (\gamma c)^n + K_M \phi k_+ (c_0 - c)(\gamma c)^m$ for the former and $-\frac{dc}{dt} = nK_N k_+ (\gamma c)^n + mK_M \phi k_+ (c_0 - c)(\gamma c)^m + (k_+ \gamma c - k_-)c_p$ for the latter, where K_M and K_N are the equilibrium constants for "heterogeneous" and homogeneous nucleation respectively, k_+ and k_- describe the rates of monomer addition and removal, γ is the activity coefficient of the monomer, c_0 and c are the monomer concentrations at time zero and time t, and ϕ is a scaling factor for the number of effective sites for nucleation. The result, the authors note, is a five parameter model to describe the polymerization process. Also, the authors use (we infer) the term "heterogeneous nucleation" in the dictionary sense of heterogeneous meaning the nucleation of "different" species, that is, new polymers growing on the surface of existing polymers. Elsewhere we note that heterogeneous nucleation has been traditionally used in the nucleation literature to indicate nucleation in a (typically solid) phase while the reactants are in a different (typically liquid) phase (23). The opinion that "heterogeneous nucleation" is actually seeded autocatalytic surface growth; other issues such as the term "extreme autocatalysis" are also addressed in our review elsewhere (23). 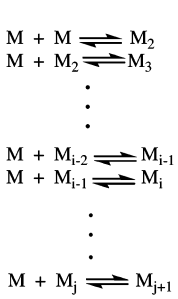
	(29)	1985	Kinetics of Sickle Hemoglobin Polymerization	
6	(18)	1983	Polymerization of Actin and Actin-like Systems: Evaluation of the Time Course of Polymerization in Relation to the Mechanism	Frieden and Goddette examined the earlier mechanisms of Oosawa (entry 1) and Wegner (entry 4) using numerical integration techniques; again, the basic mechanism of reversible subsequent monomer as shown on the right is employed in this case for the polymerization of actin. Their findings are that the Oosawa and Wegner equations are adequate for simple polymerization processes, but not for the more complex, more realistic processes of aggregation. Thus the authors added an additional step into the subsequent monomer addition mechanism. Their additional step described as  is a step prior to polymerization and involves activation of the monomer. In the case of actin, this reversible step represents ligand binding to a metal followed by a protein conformational change. 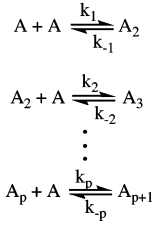

Table 1 (Continued)

Entry	Reference	Year	Title	Key Selected Contents
7	(25)	1983	On One-Dimensional Nucleation and Growth of "Living" Polymers I. Homogeneous Nucleation	$M_1 + M_1 \underset{k_2}{\overset{k_1}{\rightleftharpoons}} M_2$ $M_1 + M_2 \underset{k_4}{\overset{k_3}{\rightleftharpoons}} M_3$ ⋮ $M_1 + M_n \underset{k_{n+2}}{\overset{k_{n+1}}{\rightleftharpoons}} M_{n+1}$ This classic set of papers investigates the one-dimensional homogeneous nucleation and growth or elongation, and proposes the subsequent monomer addition mechanism for "living" polymers shown to the left. The following assumptions are also employed: i) there is only successive addition of monomers, ii) there is no geometric difference between any of the M_i, iii) $k_i=k'$ up to the critical nucleus and $k_1=k$ past the critical nucleus, where k and k′ result from the two time constants of τ and τ′, iv) a prior equilibrium exists up to the critical nucleus, and v) both reversible and irreversible growth are treated beyond the critical nucleus. Using the proposed general mechanism of successive monomer addition, four separate cases of initial rate, steady state, approaching equilibrium, and quasi-steady state are treated giving equations for nucleation for each of the four cases and an expression for reversible growth, $\frac{-dM_1}{dt} = (k_f C - k_r)^2 c_n t$, where M_1 is the monomer, k_f and k_r are the forward and reverse rate constants, C is the monomer concentration, and c_n is the critical nucleus. This expression for growth comes from employing the assumptions that all forward and reverse rate constants are equal and if the monomer concentration is constant. Lacking in this 1983 work is a test of the proposed mechanism and equations by fitting experimental data, although this is a more general treatment with good insights for one-dimensional growth, in our opinion.
	(26)	1983	On One-Dimensional Nucleation and Growth of "Living" Polymers II. Growth at Constant Monomer Concentration	
8	(27)	1986	Cooperative Polymerization Reactions: Analytical Approximations, Numerical Examples, and Experimental Strategy	Goldstein and Stryer use the simple model shown to the left for stepwise addition and subtraction of monomers to one end of a polymer, where A_1 is the monomer, A_n is the polymer of length n, k_+ and k_- are the forward and reverse rate constants prior to the formation of the seed, s, g_+ and g_- are the rate constants after the formation of the seed, and the seed size is defined as the length s, where the kinetic rate constants change. In other words, the first equation represents nucleation and the second, growth. The corresponding rate equations are then given as: $\frac{dA_n}{dt} = k_+ A_1(A_{n-1} - A_n) + k_-(A_{n+1} - A_n)$ when $A_1 + A_n \underset{k_-}{\overset{k_+}{\rightleftharpoons}} A_{n+1}$ $n < s$ $n < s$ and $\frac{dA_n}{dt} = g_+ A_1(A_{n-1} - A_n) + g_-(A_{n+1} - A_n)$ when $n > s$. The above rate equations are $A_1 + A_n \underset{g_-}{\overset{g_+}{\rightleftharpoons}} A_{n+1}$ $n \geq s$ then transferred into a dimensionless, more mathematically convenient but less physically obvious form using the assumptions of i) monomer concentration changes only by the addition or subtraction of monomer, ii) polymer formation by seed production is irreversible, and iii) the ratio of the concentration of the seed-minus-one-length to the (s-1) power of monomer concentration is essentially constant, yielding: $\frac{d\alpha_1}{d\tau} = C - C\alpha_1$ and $\frac{dC}{d\tau} = K\alpha_1^{s-1}(\alpha_1 - 1)$, where $\alpha_n = g_+/g_- * A_n$, $\tau = g_- t$, $C = \Sigma_{n-s+1}^{\infty}\alpha_n$, and "K is usually taken from equilibrum constants, but its exact value is immaterial for our discussion." A couple of important insights are apparent from the dimensionless form of the equation: first, the assumption of irreversible polymerization is justified since the same kinetic curves are observed with and without the approximation, except in the case of low concentration and long measurement time; second, the appearance of dimer, trimer, and tetramer species following the loss of monomers is apparent from simulations. Lacking, however, are a test of the proposed mechanism and its corresponding dimensionless equations using experimental data. The lack of dimensional forms of the key equations have also probably contributed to the lack of use of these equations by others who might be more interested in the underlying physical picture and main concepts behind protein aggregation.

Table 1 (Continued)

Entry	Reference	Year	Title	Key Selected Contents
9	(59)	1996	Prionics or the Kinetic Basis of Prion Diseases	This paper discusses the possibility of two different mechanisms for the formation of pathogenic prion species. The first of which is a condensed verion of Prusiner's (60,61) so-called "linear autocatalysis" mechanism shown on the right where F_A is the constant metabolic formation of A, A is the normal form of the host protein, B is the pathogenic form of A, K_M is the Michaelis constant, k_T is the turnover number, k_{-A} is the metabolic decomposition of A, k_{-B} is the metabolic decomposition of B, k_{AB} and k_{BA} are the noncatalytic conversion of A to B and B to A. From Prusiner's condensed mechanism the corresponding rate equation is obtained: $\frac{d[A]}{dt} = F_A - k_{-A}[A] - k_{AB}[A] - \frac{k_T[A]}{K_M + [A]}[B]$. Also discussed is Lansbury's (62,63,64,65,66) "passive autocatalysis mechanism" proposed for both the aggregation of prions and the plaque formation in Alzheimer's disease, $A \underset{k_{BA}}{\overset{k_{AB}}{\rightleftharpoons}} B \underset{k_D}{\overset{k_F[B]}{\rightleftharpoons}} B_2 \underset{k_D}{\overset{k_F[B]}{\rightleftharpoons}} \cdots \underset{k_D}{\overset{k_F[B]}{\rightleftharpoons}} B_n \underset{k_D}{\overset{k_F[B]}{\rightleftharpoons}} B_p$, where A is again the normal form of the host protein, B is the pathogenic monomeric form of A, B_2, B_n, and B_p are the aggregate forms of B, k_{AB} and k_{BA} are again the noncatalytic conversion of A to B and B to A, k_F is the formation rate constant, and k_D is the dissociation rate constant. Neither mechanism can be ruled out in terms of the formation of aggregates of prion proteins, and both remain as possible valid mechanisms. Also, the authors specifically state, "The aim of this paper is not a quantitative *description* of real data, but rather an *understanding* of the principles that control reality." Accordingly, this classic work has apparently not been used to treat raw kinetic data.
10	(35)	2000	Conformational Transitions and Fibrillation Mechanism of Human Calcitonin as Studied by High-Resolution Solid-State ^{13}C NMR	Saitô and coworkers suggest a mechanism for the fibrillation of the human calcitonin hormone with these three steps shown on the right where n_0 represents micellular intermediates of the same aggregation number, A_{n0} is the micellular aggregates made up of n_0 monomers of the protein, B_{n0} is the nucleus, and B_n and B_{n+1} are the elongated fibrils with n and n + 1 molecules of the protein. The corresponding analytical form of the mechanism was obtained using the three assumptions of: monomer and micelle states give the same measurable signal, the total monomer concentration is always much higher than the critical micelle concentration, and each B_n can act as a catalytic site for the conversion of A to B is represented by the following equation $f = \frac{\rho\{\exp[(1+\rho)kt] - 1\}}{\{1 + \rho\exp[(1+\rho)kt]\}}$, where f is the fraction of calcitonin in the fibrillar form and ρ represents the dimensionless value to describe the ratio of k_1 to the convoluted k which is equal to $k_2*[A]_0$. The fractional integrated rate equation is then used to fit the calcitonin aggregation data under various concentration and pH conditions. Although not readily apparent, not recognized by the authors, and not heretofore demonstrated, herein we show that Saitô and coworkers' above fractional form of the integrated equation for their 3-step mechanims turns out to be equivalent to the earlier, 1997 Finke-Watzky 2-step mechanism of nucleation followed by autocatalytic growth mechanism (31), $[A]_t = \frac{\frac{k_1}{k_2} + [A]_0}{1 + \frac{k_1}{k_2[A]_0} e^{(k_1 + k_2[A]_0)t}}$, an important insight of the present contribution. (The mathematical derivation proving this equivalence is provided in the Supporting Information.)

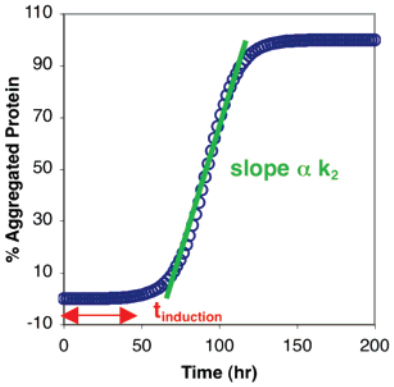

FIGURE 1: A typical kinetic curve seen for the F−W, 2-step mechanism in Scheme 1 with representative rate constants of $k_1 = 1 \times 10^{-5}$ h^{-1}, $k_2 = 1 \times 10^{-3}$ mM^{-1} h^{-1} (i.e., rate constants chosen for the sake of illustration but which are also within the range of values we will find for the protein agglomeration examples which follow). Two useful facts about this example sigmoidal curve is, as shown in the curve, k_1 (units of h^{-1}) is proportional to the inverse of the induction period time, $t_{induction}$ (units h[1]); that is, $k_1 \propto 1/t_{induction}$ and gives quantitative information about the nucleation period (also called the induction period or lag phase[1]). In addition, $k_2[A]_0$ (units h^{-1}) is proportional to the normalized slope of the line following the induction period, $+d[B]/dt \times 1/[A]_0$ (units h^{-1}) (*31*, *54*).

herein. Equation 3 is readily derivable from eq 2 in the case where one has a clean reaction, A → B, with associated clean mass balance, $[A]_t = [A]_0 - [B]_t$. Substitution for $[A]_t$ into eq 2 and solving for $[B]_t$ yield eq 3.

$$[B]_t = [A]_0 - \frac{\frac{k_1}{k_2} + [A]_0}{1 + \frac{k_1}{k_2[A]_0}\exp(k_1 + k_2[A]_0)t} \quad (3)$$

MATERIALS AND METHODS

Selection of Data Sets for Analysis. The literature was searched, using both SciFinder Scholar and the Web of Science, for the protein aggregation studies relevant to the neurodegenerative disorders, Alzheimer's, Parkinson's, and Huntington's diseases; for this first study prion related diseases were deliberately, albeit arbitrarily, omitted from the literature search in order to keep the number of papers examined to ≤100. (We are constructing a separate review and kinetic analysis of the prion protein aggregation literature and will report on that separately in due course.) The searches were then narrowed to articles containing usable protein aggregation versus time kinetic data resulting in a representative 14 data sets are presented below.

Data Analysis and Curve Fitting. Data were extracted (digitized) from published kinetic curves using Engauge Digitizer 2.12. In 13 of the 14 data sets, the data were displayed as the formation of product (B) versus time (t), and these digitized data sets were fit by the analytical equation shown in eq 3 using the nonlinear least-squares curve-fitting program in OriginLab Corporation's Origin version 7.0. In one case (see Figure 6a), the kinetic data were reported as the loss of monomeric protein (A) versus time (t); in this case, the kinetic data were fit using eq 2 and, again, Origin version 7.0. The derivation of the analytical eq 3 is given in the Supporting Information.

In the fits presented in Figures 2−12 and summarized in Table 2, we have by necessity assumed that all forms of kinetic measurement used previously in the literature *are directly proportional to the percent of aggregated protein.* This is the same assumption underlying virtually all the protein agglomeration kinetic studies to date, but is an assumption that we note merits reinvestigation in future studies. For example, changes in protein conformation, without aggregation, may also influence fluorescence, circular dichroism (CD), absorption, and dynamic light scattering (DLS), even though many papers in the relevant literature do not account for these contributions. Furthermore, for these first studies we have again by necessity assumed that the data measured by fluorescence, CD, and absorption are ideal: that is, it is assumed that there is no absorption for the monomer at the wavelength measured, and no deviation from Beer's law, so that the absorption present is due to the aggregated protein. This appears to be true for the cases where the spectra are shown (*4*, *6*, *7*, *13*), but in some cases the monomer-alone spectrum is not provided to the reader (*5*, *8*−*10*), so that we were unable to verify (or refute) this, again at present necessary, assumption. The resultant signal intensity vs time may, therefore, not necessarily be a direct measure of the aggregated protein[4] (*36*, *37*), but for the purposes of the initial treatments herein we assume that it is. It should also be noted that in the literature cases presented herein, the protein generally begins in an *unfolded or misfolded* state, either natively or by denaturation, prior to measurements of the kinetics of protein aggregation.

RESULTS AND DISCUSSION

To start, the literature was searched for protein aggregation kinetic data sets as detailed in the Materials and Methods. Both Scifinder Scholar and Web of Science were employed to search for kinetic aggregation data relevant to the neurodegenerative disorders Parkinson's disease, Alzheimer's disease, and Huntington's disease. A total of 14 representative kinetic data sets were found (*4*−*14*) encompassing four main categories of proteins: (i) amyloid-β, the peptide that is hypothesized to be central to Alzheimer's disease (*1*), (ii) α-synuclein, the peptide hypothesized to be key in Parkinson's disease (*2*), (iii) polyglutamine, the peptide hypothesized to be crucial in the etiology of Huntington's disease

[4] In the case of dynamic light scattering, there is not a simple correlation between the observed light scattering and the amount of aggregated protein; instead, the relationship is more complex. Assuming particles all of identical size, the following equation shows that the scattering intensity, $R(Q)$, is dependent upon the particle concentration, C_p (g/L), the molar mass of the particles, M_p (g/mol), the particle form factor, $P(Q)$, and the structure factor of the dispersion, $S(Q,C_p)$,that is: $R(Q) \cong KC_pM_pP(Q)\ S(Q,C_p)$ (where K is a constant dependent upon the instrumentation and difference in refractive index of particles and solvent). This can also be thought of in a more simplified way: dynamic light scattering measurements depend upon Brownian motion and the speed at which particles move (the diffusion of the molecules), and therefore the molecular weight of the polymer species can be determined by the Einstein−Stokes relation: $M = 4\pi r^3 N_A/3v$, where M is the molecular weight of the polymer, r is the radius, N_A is Avogadro's number, and v is the partial specific volume of the polymer molecule. This implies that diffusion is inversely proportional to the cubic root of the molecular weight rather than the concentration in solution. This in turn means that light scattering measurements are not directly proportional to the concentration of the solution being measured.

(*3*), and (iv) other amyloidogenic proteins not belonging to the previous three categories.

Each kinetic data set was in turn analyzed by the F−W 2-step mechanism given in Scheme 1. The results are presented in Figures 2−4, 5a−c, 6a,b, and 7−12, with Table 2 summarizing the nucleation, k_1, and growth, k_2, rate constants obtained from the kinetic analyses. The fit shown in Figure 12 overestimates the second half of the data; for this reason the data was also analyzed by the 3- and 4-step, expanded versions of the F−W mechanism which include bimolecular agglomerative growth, B + B → C (rate constant k_3) and a novel, only recently discovered autocatalytic agglomeration step, B + C → 1.5C (rate constant, k_4) (*32*). For further information on these fits the interested reader is referred to the Supporting Information (see Figure S7 and the section titled Alternative Mechanisms Considered: the 3- and 4-Step Mechanisms). Interestingly, the 2-, 3-, and 4-step fits all give similar residual values. On the basis of Ockham's razor, the fit to the simpler 2-step mechanism was chosen for presentation in Figure 12 and since *at present* there is no compelling evidence to expand the mechanism to the 3- or 4-step variants of the original, 1997 F−W mechanism.

Fitting Amyloid β Aggregation Literature Data to the 2-Step F−W Mechanism. The aggregation of proteins to form β-sheet rich amyloid fibrils has been hypothesized to be intimately involved in more than 20 human diseases (*13*, *38*). One very important amyloidogenic protein is amyloid β, which forms plaques hypothesized to be a crucial component of Alzheimer's disease (*39*). Shown in Figures 2−6 are the digitized data from the literature on aggregation of amyloid β protein along with the curve-fits to the F−W 2-step mechanism (*31*) of slow, continuous nucleation plus subsequent autocatalytic surface growth. In all cases the fits are very good if not excellent.

Fitting α-Synuclein Aggregation Literature Data to the 2-Step F−W Mechanism. The aggregation of α-synuclein has been hypothesized to be a crucial component in Parkinson's disease (*2*). Figures 7 and 8 illustrate the fits of the F−W mechanism to the aggregation of α-synuclein. Figure 7 in particular is a striking demonstration of how well the simple 2-step F−W mechanism fits the α-synuclein aggregation—that is, the nucleation and autocatalytic growth—kinetic data.

There is also some kinetic data in the literature that looks at the aggregation of α-synuclein as a function of added seed protein. The interested reader is referred to Figures S9 and S10 of the Supporting Information for the digitized data and corresponding fits.

Fitting Polyglutamine Aggregation Literature Data to the 2-Step F−W Mechanism. Aggregation of polyglutamine has been hypothesized to be intimately involved in the neurodegenerative disorder Huntington's disease (*3*). Figures 9 and 10 show the correlation between the aggregation of polyglutamine data and the fit to the F−W 2-step mechanism demonstrating a third example of protein aggregation kinetic data that can also be fit and deconvoluted into its nucleation (k_1) and autocatalytic surface growth (k_2) components by the 2-step F−W mechanism.

Wetzel has also examined the aggregation kinetics of polyglutamine in the presence of a 5% (w/w) seed (*12*). This digitized and fit data set is contained in Figure S8 of the Supporting Information for the interested reader.

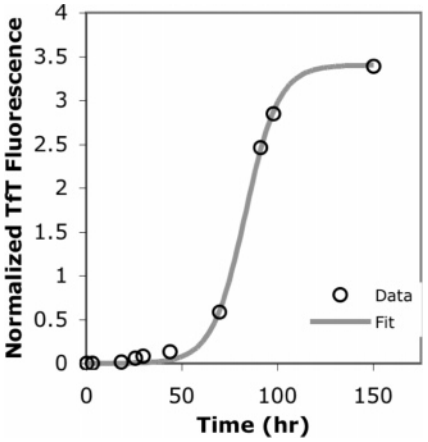

FIGURE 2: Digitized data of Kelly and co-workers' (*4*) amyloid β peptide aggregation measured (and normalized by the authors) by TfT fluorescence and fit to the F−W 2-step mechanism. Amyloid β peptide aggregation has been hypothesized to be central in the pathology of Alzheimer's disease (*1*). The fit values for this dataset are $k_1 = 8(3) \times 10^{-6}$ h^{-1} and $k_2 = 3.4(1) \times 10^{-2}$ μM^{-1}·h^{-1}.

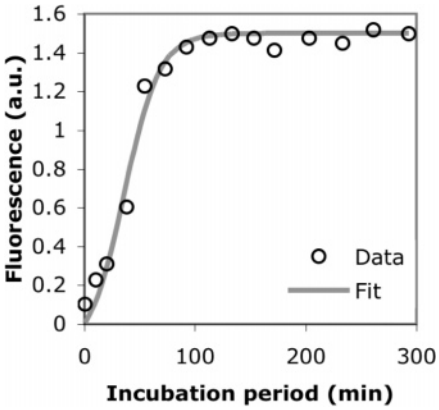

FIGURE 3: Digitized data of Vestergaard and co-workers' (*5*) aggregation of amyloid β (Aβ-42) peptide measured by ThT fluorescence and fit to the F−W 2-step mechanism. Again aggregation of this peptide is believed to be key in Alzheimer's disease (*39*). Although there is considerably less sigmoidal character to this data set (e.g., vs Figure 1), the fit is still quite good. The resultant $k_1 = 6(2) \times 10^{-3}$ min^{-1} and $k_2 = 3.8(8) \times 10^{-2}$ μM^{-1}·min^{-1}.

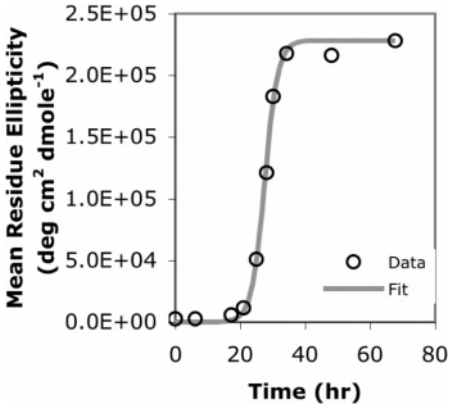

FIGURE 4: Data of Lynn and co-workers' (*6*) amyloid β peptide aggregation measured by circular dichroism (CD) digitized, and fit to the F−W 2-step mechanism. This data set and fit provide a third example of the excellent fit by the F−W mechanism to protein aggregation related to the etiology of Alzheimer's disease (*39*). The observed $k_1 = 6(7) \times 10^{-7}$ h^{-1} and $k_2 = 2.2(2) \times 10^{-6}$ mM^{-1}·h^{-1}.

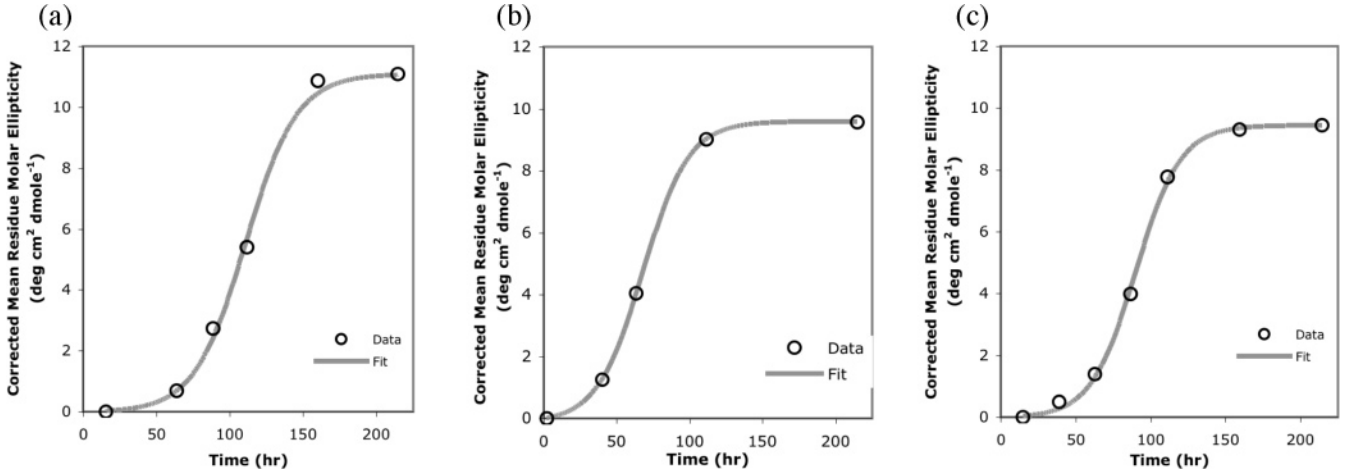

FIGURE 5: Digitized data of Lynn and co-workers' (*7*) amyloid β peptide measured as a function of added Zn^{2+} and fit to the F−W 2-step mechanism. The authors speculate that Zn^{2+} binding sites exist along the β sheets of amyloid β peptides; therefore, they measured the aggregation as a function of added [Zn^{2+}] and observed a reduced nucleation time with increased [Zn^{2+}]. The data in this figure are corrected for the negative values of ellipticity that were reported in the original reference by normalizing the data to have a minimum value of zero (*7*). By making the assumption that the negative ellipticity values, resulting from the difference in absorption of left vs right circularly polarized, would remain constant throughout a blank sample, a constant value was added to each data point shown so as to render positive all the corrected values. (For the raw, uncorrected data and fits please see Figure S1 of the Supporting Information.) Part (a) is for 1 mM of the peptide alone with $k_1 = 1.0(5) \times 10^{-4}$ h^{-1} and $k_2 = 5.1(5) \times 10^{-3}$ mM^{-1}·h^{-1}, (b) is for [Zn^{2+}]:[peptide] of 0.2 with $k_1 = 8.3(3) \times 10^{-4}$ h^{-1} and $k_2 = 6.55(9) \times 10^{-3}$ mM^{-1}·h^{-1}, and (c) represents a [Zn^{2+}]:[peptide] of 0.4 with $k_1 = 1.6(4) \times 10^{-4}$ h^{-1} and $k_2 = 7.1(4) \times 10^{-3}$ mM^{-1}·h^{-1}. A plot of the resultant k_1 and k_2 values vs [Zn^{2+}], provided as Figure S2 of the Supporting Information, shows little to no effect of the [Zn^{2+}] on the k_1 and k_2 values in this specific case.

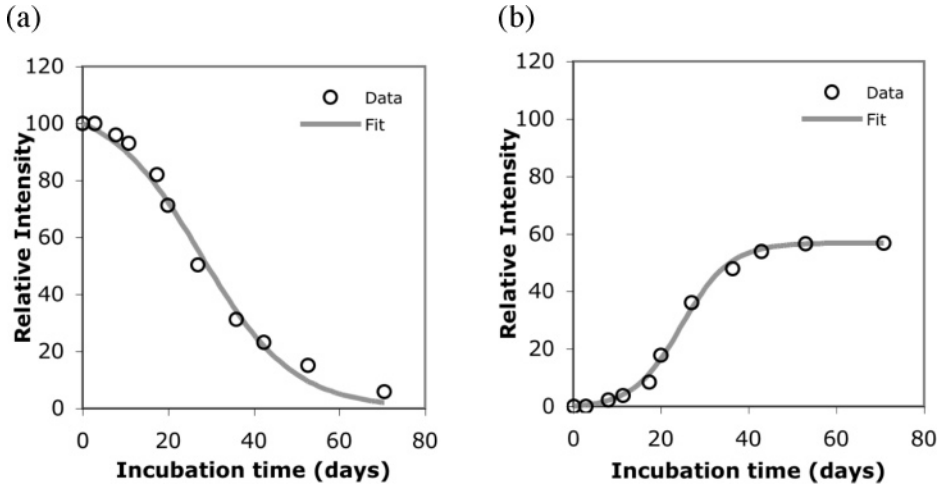

FIGURE 6: Digitized data of Rebuffat and co-workers' (*8*) amyloid β peptide aggregation measured by reversed-phase HPLC with absorbance detection plus the fits to the F−W 2-step mechanism. Part (a) is for Aβ1−16, the first 16 peptides of amyloid β ($k_1 = 7(1) \times 10^{-3}$ day^{-1}, $k_2 = 9(4) \times 10^{-4}$ mM^{-1}·day^{-1}) and (b) Aβ5−16, peptides 5−16 of amyloid β, ($k_1 = 2.1(5) \times 10^{-3}$ day^{-1} and $k_2 = 3.1(2) \times 10^{-3}$ mM^{-1}·day^{-1}).

Fitting Other Amyloidogenic Proteins Aggregation Literature Data to the 2-Step F−W Mechanism. Figures 11 and 12 show, respectively, the fits of the F−W mechanism to the aggregation of β2-microglobulin and human lysozyme proteins.

In summation to this point, all 14 data sets found by our literature search fit the F−W 2-step mechanism with an R^2 value ≥ 0.98 (Table 2). This includes data obtained by four different methods, for three different proteins, by nine different labs and spanning over four publication years. The fits are generally good, and in many cases excellent (e.g., Figures 2, 4, 6, 7, 9, and 11). *As such, this contribution is the current record of the widest set of protein aggregation data best fit by the also simplest kinetic model to date*. The implied conclusion is, therefore, that at least phenomenologically speaking, the F−W 2-step mechanism of nucleation and autocatalytic growth is a previously unrecognized, "Ockham's razor" (*34*)/*minimalistic model* for deconvoluting protein agglomeration nucleation, k_1, from (autocatalytic) growth, k_2.

The Relationship between a Generalized Form of the 1997 F−W Mechanism and the 2000 Saitô and Co-workers (35) Mechanism. Upon studying the protein aggregation literature and constructing Table 1 (vide supra), we encountered Saitô and co-workers' 2000 paper and 3-step mechanism, Scheme 3 (*35*). After some reflection, we in turn wondered if the 2-step F−W mechanism (Scheme 2) and Saitô and co-workers' 3-step mechanism might not be more closely similar than initially meets the eye (i.e., and after the three assumptions and simplification made by Saitô and co-

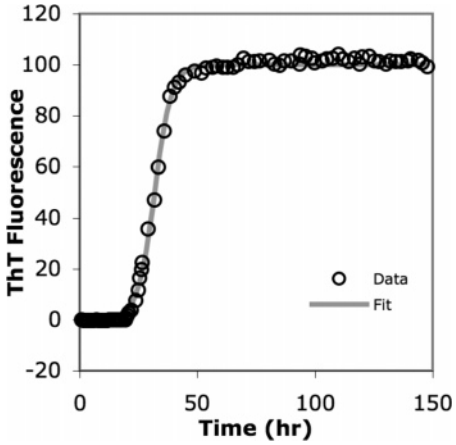

FIGURE 7: Digitized data of Fink's (*9*) α-synuclein aggregation, in the presence of macromolecular crowding induced by 100 mg/mL poly(ethylene glycol)-3350 and monitored by ThT fluorescence, and curve-fit to the F−W 2-step mechanism, $k_1 = 4.0(8) \times 10^{-5}$ h^{-1}, $k_2 = 2.77(7) \times 10^{-3}$ μM^{-1}·h^{-1}. Fink notes about α-synuclein aggregation, "The in vitro kinetic studies of α-synuclein fibril formation show an initial lag phase followed by an exponential growth phase and a final plateau..." (*9*). These are, again, the kinetic signatures of the F−W 2-step mechanism.

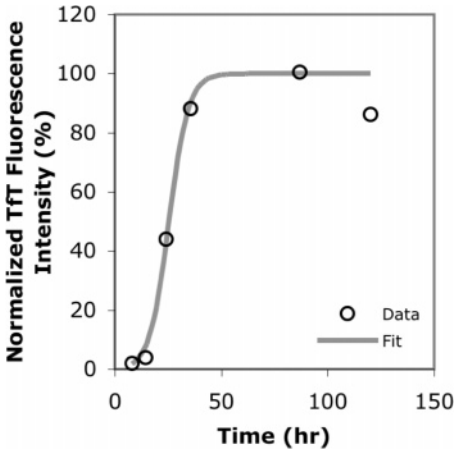

FIGURE 8: Digitized data of Sode and co-workers' (*10*) α-synuclein aggregation measured by TfT fluorescence assay analysis and fit to the F−W 2-step mechanism. The resultant $k_1 = 1(1) \times 10^{-3}$ h^{-1} and $k_2 = 2.2(6) \times 10^{-3}$ μmol^{-1}·h^{-1}.

workers, listed in Table 1, modifications those authors found necessary to simplify the mathematics into an equation usable for fitting experimental data). Indeed, in the Supporting Information *we demonstrate the mathematical identity of the F−W and Saitô analytic equations*. This means that the 3-step mechanism proposed by Saitô and co-workers in 2000 reduces to the 2-step, 1997 F−W mechanism.

In addition, one can also see intuitively how the two mechanisms shown in Schemes 2 and 3 can lead to the same overall kinetic expression. For the case of a fast prior equilibrium that lies predominantly back to the left (toward A) in the Saitô et al. mechanism, their k_{obs}'' will equal $k_1''K_{eq}''[A]^{n-1}$ which in turn will equal k_1 of the F−W mechanism, that is, $k_{obs}'' = k_1''K_{eq}''[A]^{n-1} = k_1$ (where we have substituted a simple "*n*" for Saitô's "n_0" (*35*)). That is, Saitô and co-worker's postulated pre-equilibrium of *n*A monomers to an A_n micellular-like aggregate—which others would just call soluble protein oligomers (*40*, *41*)—can be hidden within the k_1 of the F−W mechanism.

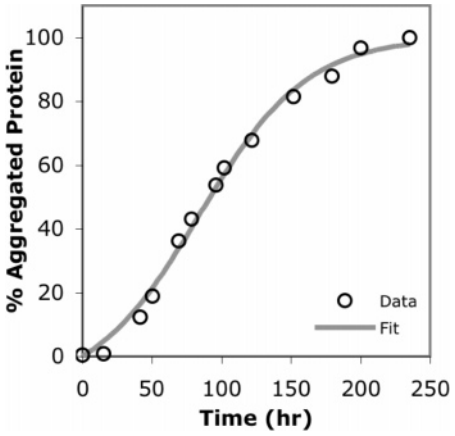

FIGURE 9: Digitized data of Wetzel and co-workers' (*11*) aggregation of polyglutamine monitored by light scattering and fit to the F−W 2-step mechanism with resultant rate constants, $k_1 = 2.6(3) \times 10^{-3}$ h^{-1} and $k_2 = 2.3(2) \times 10^{-4}$ μM^{-1}·h^{-1}.

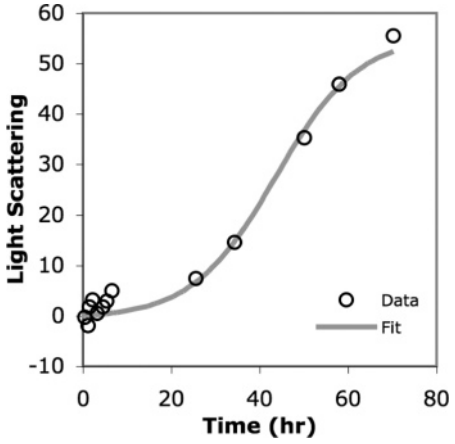

FIGURE 10: Digitized data of Wetzel's (*12*) polyglutamine aggregation without seeding monitored by light scattering and fit to the F−W 2-step mechanism. The fit values are $k_1 = 1.0(4) \times 10^{-3}$ h^{-1} and $k_2 = 1.9(2) \times 10^{-3}$ μM^{-1}·h^{-1}.

The mathematical identity of the F−W 2-step mechanism with the Saitô et al. 3-step mechanism (i.e., and post the assumptions Saitô et al. necessarily made to yield an equation that would allow them to analyze their protein aggregation kinetic data) means that, therefore, the Saitô et al. 3-step mechanism is, in the final analysis, a reinvention of the 2-step mechanism. It should, therefore, be replaced by the 2-step F−W mechanism. This comment is not intended to downgrade in any way the independent derivation and contribution by Professor Saitô and his co-workers; indeed, the fractional conversion ("*f*") form of the equation given back in Table 1 is a convenient form for analyzing data (with units of reciprocal time). Moreover, it is entirely possible that the 3-step mechanism in Scheme 3 may well eventually prove to be a more accurate description of the underlying, true protein aggregation process in at least some cases.

Relevant here is a brief discussion of the original A → B, A + B → 2B and more generalized form, *n*A → B_n, A + B_n → B_{n+1} (Scheme 4), of the F−W 2-step mechanism. In Schemes S2 and S3 of the Supporting Information we show the mathematical relationship between these two. At the first level of approximation, they are equivalent with the generalized form of the equation introducing a statistical factor into k_1' and k_2'; that is, k_1 and k_2 of the original F−W mechanism are proportional, respectively, to $(n + 1)k_1'[A]^{n-1}$ and $(n +$

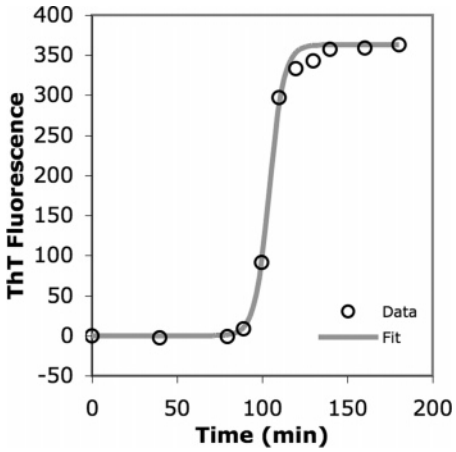

FIGURE 11: Digitized data of Goto and co-workers' (*13*) ultrasonification-induced aggregation of β2-microglobulin monitored by ThT fluorescence and fit (solid line) to the F−W 2-step mechanism. β2-Microglobulin is an amyloid protein that causes amyloidosis resulting in the deposition of amyloid fibrils in the synovia of the carpal tunnel in patients who have been receiving dialysis for more than 10 years (*67*). Note the generally excellent fit to this highly sigmoidal, approaching step-function-like kinetic curve. The fit values are $k_1 = 1(3) \times 10^{-11}$ min^{-1} and $k_2 = 6(1) \times 10^{-4}$ min^{-1}·μM^{-1}.

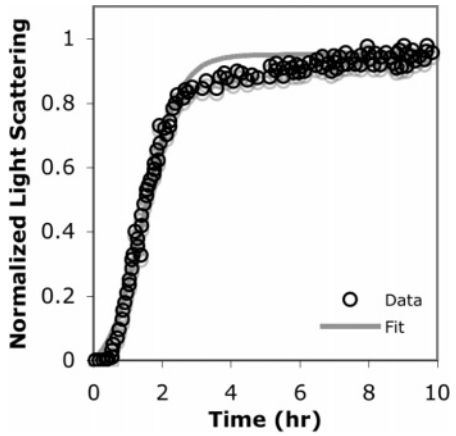

FIGURE 12: Digitized data of Dobson and co-workers' (*14*) in vitro D67H human lysozyme variant used to study the folding and misfolding of the protein, the latter leading to aggregate formation and amyloid disease, again with fits to the F−W 2-step mechanism. In 1993 the D67H lysozyme variant was discovered to be associated with a hereditary form of nonneuropathic systemic amyloidosis that causes amyloid deposits to form in various organs of the body (*68*). The aggregation data was measured by dynamic light scattering and normalized by the authors. The resultant $k_1 = 1.1(1) \times 10^{-1}$ h^{-1}, $k_2 = 1.9(1)$ μM^{-1}·h^{-1}.

1)k_2' of the generalized F−W mechanism under the conditions and assumptions of the derivation in the Supporting Information. In both k_2 and k_2' there is also a previously introduced (*31*) "scaling factor" of $(1 + \chi_{\text{growth}})/2$ for *spherical growth*, as further defined and discussed elsewhere (*31*) due to the increasing surface area of B onto which aggregation is taken to be increasingly likely as the aggregate grows. More recent (*42*) and upcoming (*43*) papers discuss a treatment of the scaling factor that is continuous with time and, therefore, allows a continuous correction to the changing fraction of B on the particle or aggregates's surface, although the specific treatment given is for the case of transition-metal nanoparticles (*42*, *43*)—one, however, that should be readily extendable by analogy to protein aggregation.

Does the F−W 2-Step Mechanism Make Physical Sense for Protein Aggregation? The good to excellent fits obtained for a wide range of protein aggregation data (Figures 2−12) argue that the F−W mechanism must be portraying at least some of the key features of the more complete, elementary step process of protein agglomeration. Nevertheless, the good fits still beg the question of "does the F−W mechanism make physical sense for protein aggregation?" A closely related question is what is a deeper physical description of "A" and "B" in the 2-step mechanism, A → B, A + B → 2B?

In their simplest forms, A is just the predominant form of the unfolded or misfolded, ready-to-aggregate protein in solution while B is more complex, B representing the protein aggregates, with all different sizes of B at a given time, *t*, being lumped into one average "B". Physically, B appears to be (growing) *surface area* of the aggregated protein, that is, the surface area that is primarily involved in, and leads to, aggregation as $A + B_n \rightarrow B_{n+1}$ grows to higher *n*. This is consistent with the description by Fink et al. in the case of α-synuclein where he describes "a partially folded intermediate is anticipated to have contiguous hydrophobic patches on its surface, which are likely to foster self-association and hence potentially fibrillation" (*44*)—an apt description of our "B". The broad descriptor "B" therefore covers a range anywhere from a hypothesized *toxic intermediate species* (*45*−*52*) all the way up to the hypothesized nontoxic fibril (*45*). This makes it rather apparent that much more effort needs to go into demonstrating by direct spectroscopic means what "B" is more precisely *and as a function of time*.

The Emerging Case for Protofibrils as the Toxic Intermediate(s). A consensus appears to be developing in the literature that intermediate protofibrils and/or soluble oligomers are the toxic species in neurodegenerative diseases (*45*−*52*). (For more references on intermediate protofibril and soluble oligomer species, please refer to the Supporting Information.) A very important implication of the fits to the F−W 2-step mechanism provided herein is that the *soluble monomer-to-protofibril-to-final fibril size vs time is in principle obtainable from the deconvoluted k_1 and k_2 and knowledge of the beginning protein concentration, A_0, so long as a final fibril geometry and final size are also known.* The treatment is expected to be directly analogous to that we have developed for nanocluster size vs time (*53*), but with the caveat that the shape and geometry treatment will of course be different than the treatment used for spherical nanoparticles (*53*). The needed equations are under development (*54*). In short, an implication of the fits herein deconvoluting nucleation, k_1, from surface autocatalytic growth, k_2, is that protofibril size vs time will be predictable (again, if the final geometry and average size can be firmly established). This in turn promises to greatly expedite the rational synthesis of fibrils of known size and, hence, their detailed study and all the insights those studies promise to provide.

Advantages and Especially Caveats/Limitations of the F−W 2-Step Kinetic Model. The F−W 2-step mechanism appears to fit a broad range of neurological protein aggregation data. The simplicity and quality of the fits, the deconvolution of the nucleation, k_1, from the growth, k_2, and the implications for fibril size vs time studies are all extremely valuable components of the *F−W kinetic model.*

Table 2: Rate Constants and Coefficient of Determination (R^2) Values from Fitting 14 Literature Protein Aggregation Kinetic Data Sets to the F−W 2-Step Mechanism, Scheme 2, Vide Supra (The Plots of Those Fits Are Shown in Figures 2−12)[a]

entry	reference	system	distinguishing experimental details	data collection method	k_1[a]	k_2[a,b]	R^2 [c]
1	Kelly (*4*)	amyloid β		fluorescence	$8(3) \times 10^{-6}$ h^{-1}	$2.3(1) \times 10^{-3}$ μM^{-1} h^{-1}	0.9989
2	Vestergaard (*5*)	amyloid β		fluorescence	$6(2) \times 10^{-3}$ min^{-1}	$7(2) \times 10^{-4}$ μM^{-1} min^{-1}	0.9830
3	Lynn (*6*)	amyloid β		CD	$6(7) \times 10^{-7}$ h^{-1}	$3.0(3) \times 10^{-1}$ mM^{-1} h^{-1}	0.9971
4	Lynn (*7*)	amyloid β	1 mM peptide[d]	CD	$1.0(5) \times 10^{-4}$ h^{-1}	$5.7(6) \times 10^{-2}$ mM^{-1} h^{-1}	0.9973
5			[Zn]:[peptide] = 0.2[d]		$8.3(3) \times 10^{-4}$ h^{-1}	$6.29(9) \times 10^{-2}$ mM^{-1} h^{-1}	1.0000
6			[Zn]:[peptide] = 0.4[d]		$1.6(4) \times 10^{-4}$ h^{-1}	$6.7(4) \times 10^{-2}$ mM^{-1} h^{-1}	0.9988
7	Rebuffat (*8*)	amyloid β	Aβ1−16	absorbance	$7(1) \times 10^{-3}$ days^{-1}	$1.8(8) \times 10^{-3}$ mM^{-1} days^{-1}	0.9904
8			Aβ5−16		$2.1(5) \times 10^{-3}$ days^{-1}	$3.5(2) \times 10^{-3}$ mM^{-1} days^{-1}	0.9964
9	Fink (*9*)	α-synuclein		fluorescence	$4.0(8) \times 10^{-5}$ h^{-1}	$4.0(1) \times 10^{-3}$ μM^{-1} h^{-1}	0.9986
10	Sode (*10*)	α-synuclein		fluorescence	$1(1) \times 10^{-3}$ h^{-1}	1.1(3) μM^{-1} h^{-1}	0.9778
11	Wetzel (*11*)	polyglutamine		DLS	$2.6(3) \times 10^{-3}$ h^{-1}	$2.3(2) \times 10^{-4}$ μM^{-1} h^{-1}	0.9941
12	Wetzel (*12*)	polyglutamine		DLS	$1.0(4) \times 10^{-3}$ h^{-1}	$1.3(1) \times 10^{-2}$ μM^{-1} h^{-1}	0.9877
13	Goto (*13*)	β-microglobulin		fluorescence	$1(3) \times 10^{-11}$ min^{-1}	$9(1) \times 10^{-3}$ μM^{-1} min^{-1}	0.9968
14	Dobson (*14*)	D67H lysozyme		DLS	$1.1(1) \times 10^{-1}$ h^{-1}	$1.41(7) \times 10^{-1}$ μM^{-1} h^{-1}	0.9846

[a] The error bars are determined by the square root of the reduced χ^2 based on a modified Levenberg−Marquardt algorithm.[1] [b] The concentration units on k_2 were determined by multiplying by the maximum intensity and dividing by the initial starting concentration of the respective protein being measured. [c] R^2 is the coefficient of determination that gives information about the goodness of fit of the model applied (the closer this value is to 1.0, the more precise the fit is to the data). [d] These data points were corrected for the negative ellipticity values that were reported (vide infra).

Scheme 3: Saitô and Co-workers' (*35*) Mechanism for the Aggregation of Human Calcitonin

$$n_0A \text{ (monomers)} \overset{K_{eq}''}{\rightleftharpoons} A_{n0} \text{ (micelle)}$$

$$A_{n0} \xrightarrow{k_1''} B_{n0}$$

$$A + B_n \xrightarrow{k_2''} B_{n+1}$$

Scheme 4: The Generalized Form of the F−W Mechanism

$$nA \xrightarrow{k_1'} B_n$$

$$A + B_n \xrightarrow{k_2'} B_{n+1}$$

Another significant advantage is that the use of the 2-step F−W mechanism allows kinetic fits en route to the correct deduction of mechanism in cases where fewer data of lower precision are available (*55*). The above positives noted, the *limitations* of the F−W model also need to be clearly noted. Some main limitations apparent at present are as follows:

(1) The F−W 2-step mechanism is obviously a highly condensed, oversimplified, phenomenological *model* of the real protein agglomeration that often consists of probably hundreds if not thousands of steps. The ability of such a 2-step model to account in at least an average way for the multistep reaction is, in that sense, remarkable even if a significant oversimplification.

(2) The resultant k_1 and k_2 values are, therefore, *averages* over all of the true underlying steps. As such, important kinetic and mechanistic information must be hidden in the "average" pseudo-elementary steps (*31*) of A → B, A + B → 2B or even the more generalized nA → B$_n$, A + B$_n$ → B$_{n+1}$. Put another way, the F−W model assumes that k_1 and k_2 are independent of aggregate size (i.e., that for the nth step a given $k_n = k_{n+1} \propto k_{n+2}$ and so on). This is probably never exactly true, and in some cases may hide a very important increase or decrease in the rate of, for example, growth with aggregate particle size. Another issue here, as the kinetic equations in Scheme S2 (or just thinking about the following) make apparent, is that, during the nucleation process, [A] is approximately constant. Therefore, a higher kinetic order in [A], that is, $k_1'[A]^n$, is easily hidden kinetically and can appear as an apparent $k_{1(\text{apparent})}[A]_1$ dependence, where in fact $k_1 \propto k_1'[A]^{n-1}$. This situation is something we already have experimental evidence for in the case of transition-metal nanocluster nucleation and growth (*43*), and is something that we expect will be more common. This is actually an advantage when working up kinetic data, as fits to the simple, apparently first-order nucleation step, A → B, are seen—an advantage so long as the user is aware that further plotting of the pseudo-first-order $k_{1(\text{apparent})}$ vs [A] is needed to test for a higher order nA → B$_n$ component to the reaction.

(3) The fact that all sizes of the growing aggregate are hidden behind the general descriptor "B" is a significant weakness, given the growing evidence that smaller, intermediate size fibrils may be the more toxic species (*45*−*52*). This weakness is mitigated against somewhat by the fact that k_1 and k_2 can be used, along with a knowledge of the final geometry and final (average) size of the aggregates to obtain an (average) size vs time of the aggregates (*53*) or fibrils. Nevertheless, a better experimental handle on the sizes of "B" vs time is a very important avenue of future research.

The above are the main caveats and limitations of the F−W 2-step model that are apparent to us, at least at present. Other disadvantages (as well as other possible advantages?) will undoubtedly become apparent with time. The situation is perhaps best stated by Eigen in his analysis of prion disease kinetics (*59*): "The model chosen must be simple enough to yield lucid results. On the other hand, it must be complex enough to comprise the essential influences that characterize nucleated aggregation."

SUMMARY AND CONCLUSIONS

The main insights from this contribution are the following:

(i) Fourteen protein aggregation data sets for primarily three different proteins (amyloid β, α-synuclein, and polyglutamine) obtained by four different monitoring methods and nine individual research labs were fit to the F−W 2-step mechanism/model. The resultant fits separate and quantitate for the first time the nucleation and growth quantitative rate constants for the representative 14 data sets and under the

assumptions noted in Materials and Methods (e.g., assuming as in the prior literature that the signal intensity is directly proportional to the amount of aggregated protein).

(ii) The F−W 2-step mechanism of $A \rightarrow B$ and $A + B \rightarrow 2B$ with the generalized form, $nA \rightarrow B_n$ and $A + B_n \rightarrow B_{n+1}$, appears, therefore, to provide the simplest possible, "Ockham's razor" model for protein aggregation across a fairly wide body of data. Its most important feature is its ability to separate and quantitate nucleation from growth in a clear, well-defined, easily applied way.

(iii) The main limitations of the F−W kinetic model that are apparent at present were also noted, specifically the fact that it is an oversimplified, phenomenological model of the true, multistep process, that it provides average k_1 and k_2 values that may hide important changes in k_1 and k_2 with growing aggregate size, and that B is a catch-all for the growing aggregate which, again, will hide any important differences in the growing aggregate and protofibrils as a function of their size.

(iv) Even given its limitations, since the F−W mechanism gives separate rate constants for nucleation and growth, therapeutic opportunities are apparent. For instance, quantitative studies aimed at understanding what factors start vs stop nucleation (k_1) should in turn yield opportunities for better treatments—namely inhibiting the nucleation step and thus stopping aggregation from even beginning. The importance of mechanistic understanding to therapeutic approaches should not be underestimated; a interesting historical case backing this assertion is sickle cell hemoglobin polymerization where Eaton and Hofrichter noted: "Finally, kinetic studies have played a central role in understanding the pathophysiology of sickle cell disease and the design of strategies for therapy" (*56*).

(v) The deconvolution herein of protein aggregation into its nucleation, k_1, and autocatalytic growth, k_2, components also promises to allow more detailed studies and insights into established phenomenological linear-free-energy relationships correlating protein aggregation rates (typically after the "lag" phase; i.e., really during the k_2 growth phase) with calculated indices for hydrophobicity, charge, and intrinsic propensity to form β-sheets or α-helices (*57*) as well as extrinsic factors such as pH, ionic strength, and protein concentration (*57*). As Dobson, Chiti, and Vendruscolo (*57*) have noted, correlations for the crucial "lag" (really nucleation, k_1) phase need to be done, *and that now is possible*—that is, more rigorous correlations of *both* k_1 and k_2 values with the above intrinsic as well as extrinsic properties are now also possible.

(vi) In addition, a host of other, more detailed and more quantitative studies of protein agglomeration—that is, nucleation (k_1) and growth (k_2)—now become possible, specifically any and all desired studies looking at the factors that influence k_1 vs those that influence k_2.

(vii) Finally, an interesting hypothesis resulting from this and our other (*31*−*33*) work—indeed, the most far-reaching hypothesis to result from this work in combination with our prior work on the F−W mechanism in other areas of science (*31*−*33*)—is that the F−W mechanism appears to be a (if not *the*) more general, simplest/Ockham's razor, phenomenological kinetic model for first-order phase transitions in solution (first-order phase transitions being defined as "a change in state of aggregation of a system accompanied by a discontinuous change in enthalpy, entropy, and volume at a single temperature and pressure" (*58*)). We have shown previously that this mechanism fits nanocluster agglomeration (*31*, *32*) (see the Supporting Information for a more expanded list of nanocluster references), we have shown herein that the 2-step mechanism fits the completely different case of protein aggregation, and in other studies in progress we show that the F−W model can account for at least some solid-state kinetic data as well (*33*). The evidence to date suggests, then, that the F−W 2-step mechanism is the more general, Ockham's razor kinetic model or "mechanism" for first-order phase transitions in solution. We view and offer this as a hypothesis, one able to connect a broad spectrum of previously largely unconnected literature (*23*, *31*−*33*).

ACKNOWLEDGMENT

This project grew out of a seminar given by R.G.F. at Brandeis in November of 2005; the kind invitation from the faculty of the Brandeis Department of Chemistry, and the stimulating time at Brandeis, are a pleasure to acknowledge.

SUPPORTING INFORMATION AVAILABLE

Derivation of the analytic equation of the F−W 2-step mechanism; derivation of Saitô and co-workers' 2-step mechanism for the aggregation of calcitonin and its equivalence to the F−W 2-step mechanism; comparison of the original and generalized form of the F−W 2-step mechanism; examination of the scaling factors for the rate constants, k_1 and k_2; additional references for nanocluster formation data accounted for with the F−W mechanism; additional references for fibril intermediate species; numerical integration of kinetic data using MacKinetics; effect of added $[Zn^{2+}]$ on the rate constants of amyloid β aggregation; alternative mechanisms considered: the 3- and 4-step mechanisms; fits of amyloid β aggregation data to the 3- and 4-step mechanisms; comparison of rate constants obtained from the 2-, 3-, and 4-step mechanisms, derivation of analytic equations for autocatalysis alone and the 2-step mechanism when $[B]_0 \neq 0$; fits of polyglutamine seeded data for autocatalysis alone, the 2-step mechanism, and the 2-step mechanism with $[B]_0 \neq 0$, along with a table of resultant rate constants; fits of α-synuclein seeded data for the 2-step and 2-step with $[B]_0 \neq 0$ mechanisms with a table of resultant rate constants; correlations of the k_1 and k_2 rate constants with the $[B]_0$. This material is available free of charge via the Internet at http://pubs.acs.org.

REFERENCES

1. Blennow, K., de Leon, M. J., and Zetterberg, H. (2006) Alzheimer's disease, *Lancet 368*, 387−403.
2. Dauer, W., and Przedborski, S. (2003) Parkinson's disease: mechanisms and models, *Neuron 39*, 889−909.
3. Bates, G. P., and Benn, C. (2002) The polyglutamine diseases, in *Huntington's Disease* (Bates, G. P., Harper, P. S., Jones, L., Eds.) 3rd ed., pp 429−472, Oxford University Press, Oxford.
4. Bieschke, J., Zhang, Q., Powers, E. T., Lerner, R. A., and Kelly, J. W. (2005) Oxidative metabolites accelerate Alzheimer's amyloidogenesis by a two-step mechanism, eliminating the requirement for nucleation, *Biochemistry 44*, 4977−4983.
5. Vestergaard, M., Kerman, K., Saito, M., Nagatani, N., Takamura, Y., and Tamiya, E. (2005) A rapid label-free electrochemical detection and kinetic study of Alzheimer's amyloid beta aggregation, *J. Am. Chem. Soc. 127*, 11892−11893.

6. Lu, K., Jacob, J., Thiyagarajan, P., Conticello, V. P., and Lynn, D. G. (2003) Exploiting amyloid fibril lamination for nanotube self-assembly, *J. Am. Chem. Soc. 125*, 6391−6393.
7. Dong, J., Shokes, J. E., Scott, R. A., and Lynn, D. G. (2006) Modulating amyloid self-assembly and fibril morphology with Zn(II), *J. Am. Chem. Soc. 128*, 3540−3542.
8. Zirah, S., Kozin, S., Mazur, A. K., Blond, A., Cheminant, M., Ségalas-Milazzo, I., Debey, P., and Rebuffat, S. (2006) Structural changes of region 1−16 of the Alzheimer disease amyloid β peptide upon zinc binding and in vitro aging, *J. Biol. Chem. 281*, 2151−2161.
9. Fink, A. L. (2006) The aggregation and fibrillation of α-synuclein, *Acc. Chem. Res. 39*, 628−634.
10. Sode, K., Usuzaka, E., Kobayashi, N., and Ochiai, S. (2005) Engineered α-synuclein prevents wild type and familial Parkin variant fibril formation, *Biochem. Biophys. Res. Commun. 335*, 432−436.
11. Chen, S., Ferrone, F. A., and Wetzel, R. (2002) Huntington's disease age-of-onset linked to polyglutamine aggregation nucleation, *Proc. Natl. Acad. Sci. U.S.A. 99*, 11884−11889.
12. Wetzel, R. (2006) Kinetics and thermodynamics of amyloid fibril assembly, *Acc. Chem. Res. 39*, 671−679.
13. Ban, T., Yamaguchi, K., and Goto, Y. (2006) Direct observation of amyloid fibril growth, propagation, and adaptation, *Acc. Chem. Res. 39*, 663−670.
14. Dumoulin, M., Kumita, J. R., and Dobson, C. M. (2006) Normal and aberrant biological self-assembly: Insights from studies of human lysozyme and its amyloidogenic variants, *Acc. Chem. Res. 39*, 603−610.
15. Oosawa, F., Asakura, S., Hotta, K., Imai, N., and Ooi, T. (1959) G-F transformation of actin as a fibrous condensation, *J. Polym. Sci. 37*, 323−336.
16. Oosawa, F., and Kasai, M. (1962) A theory of linear and helical aggregations of macromolecules, *J. Mol. Biol. 4*, 10−21.
17. Wegner, A., and Engel, J. (1975) Kinetics of the cooperative association of actin to actin filaments, *Biophys. Chem. 3*, 215−225.
18. Frieden, C., and Goddette, D. W. (1983) Polymerization of actin and actin-like systems: evaluation of the time course of polymerization in relation to the mechanism, *Biochemistry 22*, 5836−5843.
19. Eisenberg, H. (1971) Glutamate dehydrogenase: anatomy of a regulatory enzyme, *Acc. Chem. Res. 4*, 379−385.
20. Thusius, D., Dessen, P., and Jallon, J.-M. (1975) Mechanism of bovine liver glutamate dehydrogenase self-association, *J. Mol. Biol. 92*, 413−432.
21. Thusius, D. (1975) Mechanism of bovine liver glutamate dehydrogenase self-assembly: II. Simulation of relaxation spectra for an open linear polymerization proceeding via a sequential addition of monomer units, *J. Mol. Biol. 94*, 367−383.
22. Jullien, M., and Thusius, D. (1976) Mechanism of bovine liver glutamate dehydrogenase self-assembly: III. Characterization of the association-dissociation stoichiometry with quasi-elastic light scattering, *J. Mol. Biol. 101*, 397−416.
23. Morris, A. M., Watzky, M. A., and Finke, R. G., A critical review of the literature and future directions towards achieving the goal of determining the mechanism of protein aggregation, in progress.
24. Bishop, M. F., and Ferrone, F. A. (1984) Kinetics of nucleation-controlled polymerization, *Biophys. J. 46*, 631−644.
25. Firestone, M. P., De Levie, R., and Rangarajan, S. K. (1983) On one-dimesional nucleation and growth of "living" polymers I. Homogeneous nucleation, *J. Theor. Biol. 104*, 535−552.
26. Rangarajan, S. K., and De Levie, R. (1983) On one-dimensional nucleation and growth of "living" polymers II. Growth at constant monomer concentration, *J. Theor. Biol. 104*, 553−570.
27. Goldstein, R. F., and Stryer, L. (1986) Cooperative polymerization reactions: analytical approximations, numerical examples, and experimental strategy, *Biophys. J. 50*, 583−599.
28. Ferrone, F. A., Hofrichter, J., Sunshine, H. R., and Eaton, W. A. (1980) Kinetic studies on photolysis-induced gelation of sickle-cell hemoglobin suggest a new mechanism, *Biophys. J. 32*, 361−377.
29. Ferrone, F. A., Hofrichter, J., and Eaton, W. A. (1985) Kinetics of sickle hemoglobin polymerization II. A double nucleation mechanism, *J. Mol. Biol. 183*, 611−631.
30. LaMer, V. K., and Dinegar, R. H. (1950) Theory, production and mechanism of formation of monodispersed hydrosols, *J. Am. Chem. Soc. 72*, 4847−4854.
31. Watzky, M. A., and Finke, R. G. (1997) Transition metal nanocluster formation kinetic and mechanistic studies. A new mechanism when hydrogen is the reductant: slow, continuous nucleation and fast autocatalytic surface growth, *J. Am. Chem. Soc. 119*, 10382−10400.
32. Besson, C., Finney, E. E., and Finke, R. G. (2005) A mechanism for transition-metal nanoparticle self-assembly, *J. Am. Chem. Soc. 127*, 8179−8184.
33. Finney, E. E., and Finke, R. G. Solid-state kinetics and the Avrami and subsequent kinetic models revisited: The Finke-Watzky 2-step nucleation and autocatalytic growth mechanism as the Ockham's razor, phenomenological mechanism for 1st-order phase transitions, in preparation.
34. William of Ockham, 1285−1349, as cited in E. A. Moody (1967) *The Encyclopedia of Philosophy*, Vol. 7, MacMillan, New York.
35. Kamihira, M., Naito, A., Tuzi, S., Nosaka, A. Y., and Saitô, H. (2000) Conformational transitions and fibrillation mechanism of human calcitonin as studied by high-resolution solid-state ^{13}C NMR, *Protein Sci. 9*, 867−877.
36. Roefs, S. P. F. M., and De Kruif, K. G. (1994) A model for the denaturation and aggregation of β-lactoglobulin, *Eur. J. Biochem. 226*, 883−889.
37. Sun, S. F. (2004) Diffusion, in *Physical Chemistry of Macromolecules: Basic Principles and Issues*, 2nd ed., pp 223−242, Wiley and Sons, New York.
38. Westermark, P. (2005) Aspects on human amyloid forms and their fibril polypeptides, *FEBS 272*, 5942−5949.
39. Golde, T. E., Dickson, D., and Hutton, M. (2006) Filling in the gaps in the Aβ cascade hypothesis of Alzheimer's disease, *Curr. Alzheimer's Res. 3*, 493−504 and references therein.
40. Kayed, R., Head, E., Thompson, J. L., McIntire, T. M., Milton, S. C., Cotman, C. W., and Glabe, C. G. (2003) Common structure of soluble amyloid oligomers implies common mechanism of pathogenesis, *Science 300*, 486−489.
41. Lomakin, A., Teplow, D. B., Kirschner, D. A., and Benedek, G. B. (1997) Kinetic theory of the fibrillogenesis of the amyloid-β protein, *Proc. Natl. Acad. Sci. U.S.A. 94*, 7942−7947.
42. Schmidt, A. F., and Smirnov, V. V. (2005) Concept of "magic" number clusters as a new approach to the interpretation of unusual kinetics of the Heck reaction with aryl bromides, *Top. Catal. 32*, 71−75.
43. Finney, E. E., Ott, L. S., Watzky, M. A., and Finke, R. G., Transition-metal nanocluster kinetic and mechanistic studies en route to nanocluster size control: additional studies of nucleation and growth, manuscript in preparation.
44. Uversky, V. N., Li, J., and Fink, A. L. (2001) Evidence for a partially folded intermediate in α-synuclein fibril formation, *J. Biol. Chem. 276*, 10737−10744.
45. Ferreira, S. T., Vieira, M. N. N., and De Felice, F. G. (2007) Soluble protein oligomers as emerging toxins in Alzheimer's and other amyloid diseases, *IUBMB Life 59*, 332−345.
46. Walsh, D. M., and Selkoe, D. J. (2007) Aβ oligomers—A decade of discovery, *J. Neurochem. 101*, 1172−1184.
47. Harper, J. D., Wong, S. S., Lieber, C. M., and Lansbury, P. T., Jr. (1999) Assembly of Aβ amyloid protofibrils. An in vitro model for a possible early event in Alzheimer's disease, *Biochemistry 38*, 8972−8980.
48. Volles, M. J., and Lansbury, P. T., Jr. (2003) Zeroing in on the pathogenic form of α-synuclein and its mechanism of neurotoxicity in Parkinson's disease, *Biochemistry 42*, 7871−7878.
49. Chromy, B. A., Nowak, R. J., Lambert, M. P., Viola, K. L., Chang, L., Velasco, P. T., Jones, B. W., Fernandez, S. J., Lacor, P. N., Horowitz, P., Finch, C. E., Krafft, G. A., and Klein, W. L. (2003) Self-assembly of Aβ(1−42) into globular neurotoxins, *Biochemistry 42*, 12749−12760.
50. Kaylor, J., Bodner, N., Edridge, S., Yamin, G., Hong, D.-P., and Fink, A. L. (2005) Characterization of oligomeric intermediates in α-synuclein fibrillation. FRET studies of Y125W/Y133F/Y136F α-synuclein, *J. Mol. Biol. 353*, 357−372.
51. Tabner, B. J., El-Agnaf, O. M. A., Turnbull, S., German, M. J., Paleologou, K. E., Hayashi, Y., Cooper, L. J., Fullwood, N. J., and Allsop, D. (2005) Hydrogen peroxide is generated during the very early stages of aggregation of the amyloid peptides implicated in Alzheimer's disease and familial British dementia, *J. Biol. Chem. 280*, 35789−35792.
52. El-Agnaf, O. M. A., Salem, S. A., Paleologou, K. E., Curran, M. D., Gibson, M. J., Court, J. A., Schlossmacher, M. G., and Allsop, D. (2006) Detection of oligomeric forms of α-synuclein protein

in human plasma as a potential biomarker for Parkinson's disease, *FASEB J. 20*, 419−425.
53. Finney, E. E., and Finke, R. G. Transition-metal nanocluster size vs. formation time: a mechanism-based treatment, in preparation.
54. Watzky, M. A., Morris, A. M., and Finke, R. G. Studies in progress.
55. Smith, S. E., Sasaki, J. M., Bergman, R. G., Mondloch, J. E., and Finke, R. G. (2008) Platinum catalyzed Sn-Ph and Sn-Me transfer to $Cp^*(PMe_3)IrCl_2$: evidence for an autocatalytic reaction pathway with an unusual preference for Sn-Me transfer, *J. Am. Chem. Soc.*, accepted for publication.
56. Eaton, W. A., and Hofrichter, J. (1990) Sickle cell hemoglobin polymerization, in *Advances in Protein Chemistry*, Vol. 40, p 159, Academic Press, San Diego.
57. DuBay, K. F., Pawar, A. P., Chiti, F., Zurdo, J., Dobson, C. M., and Venruscolo, M. (2004) Prediction of the absolute aggregation rates of amyloidogenic polypeptide chains, *J. Mol. Biol. 341*, 1317−1326.
58. (2003) McGraw-Hill Dictionary of Scientific and Technical Terms, 6th ed., p 807, McGraw-Hill, New York.
59. Eigen, M. (1996) Prionics or the kinetic basis of prion disease, *Biophys. Chem. 63*, A1−A18.
60. Prusiner, S. B. (1991) Molecular biology of prion diseases, *Science 252*, 1515−1522.
61. Cohen, F. E., Pan, K.-M., Huang, Z., Baldwin, M., Fletterick, R. J., and Prusiner, S. B. (1994) Structural clues to prion replication, *Science 264*, 530−531.
62. Jarrett, J. T., and Lansbury, Jr., P. T. (1993) Seeding "one-dimensional crystallization" of amyloid: a pathogenic mechanism in Alzheimer's disease and Scrapie?, *Cell 73*, 1055−1058.
63. Come, J. H., Fraser, P. E., and Lansbury, P. T., Jr. (1993) A kinetic model for amyloid formation in the prion diseases: importance of seeding, *Proc. Natl. Acad. Sci. U.S.A. 90*, 5959−5963.
64. Lansbury, P. T. (1994) Mechanism of scrapie replication, *Science 265*, 1510.
65. Lansbury, P. T., Jr. and Caughey, B. (1995) The chemistry of scrapie infection: implications of the 'ice 9' metaphor, *Chem. Biol. 2*, 1−5.
66. Caughey, B., Kocisko, D. A., Raymond, G. J., and Lansbury, P. T., Jr. (1995) Aggregates of scrapie-associated prion protein induce the cell-free conversion of protease-sensitive prion protein to the protease-resistant state, *Chem. Biol. 2*, 807−817.
67. Yamamoto, S., and Gejyo, F. (2005) Historical background and clinical treatment of dialysis-related amyloidosis, *Biochim. Biophys. Acta 1753*, 4−10.
68. Pepys, M. B., Hawkins, P. N., Booth, D. R., Vigushin, D. M., Tennent, G. A., Soutar, A. K., Totty, N., Nguyen, O., Blake, C. C. F., Terry, C. J., Feest, T. G., Zalin, A. M., and Hsuan, J. J. (1993) Human lysozyme gene mutations cause hereditary systemic amyloidosis, *Nature 362*, 553−557.

BI701899Y